

# RSC Advances



This is an *Accepted Manuscript*, which has been through the Royal Society of Chemistry peer review process and has been accepted for publication.

*Accepted Manuscripts* are published online shortly after acceptance, before technical editing, formatting and proof reading. Using this free service, authors can make their results available to the community, in citable form, before we publish the edited article. This *Accepted Manuscript* will be replaced by the edited, formatted and paginated article as soon as this is available.

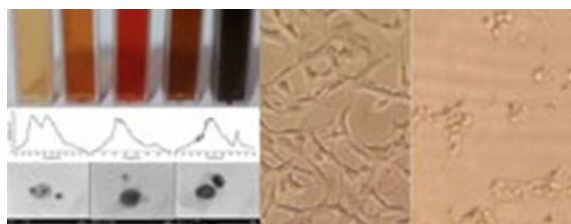
You can find more information about *Accepted Manuscripts* in the [Information for Authors](#).

Please note that technical editing may introduce minor changes to the text and/or graphics, which may alter content. The journal's standard [Terms & Conditions](#) and the [Ethical guidelines](#) still apply. In no event shall the Royal Society of Chemistry be held responsible for any errors or omissions in this *Accepted Manuscript* or any consequences arising from the use of any information it contains.

## Green synthesis of anisotropic silver nanoparticles with potent anticancer activity using *Taxus baccata* extract

Abolghasem Abbasi Kajani, Abdol-Khalegh Bordbar,\* Sayyed Hamid Zarkesh Esfahani, Ahmad Reza Khosropour and Amir Razmjou

High stable colloidal silver nanoparticles with potent anticancer activity against MCF-7 cells were synthesized using *Taxus baccata* extracts.



# Green synthesis of anisotropic silver nanoparticles with potent anticancer activity using *Taxus baccata* extract

Abolghasem Abbasi Kajani,<sup>a</sup> Abdol-Khalegh Bordbar,<sup>\*b</sup> Sayyed Hamid Zarkesh Esfahani,<sup>c</sup> Ahmad Reza Khosropour<sup>b</sup> and Amir Razmjou<sup>a</sup>

<sup>a</sup> Department of Biotechnology, Faculty of Advanced Sciences and Technologies, University of Isfahan, Isfahan, Iran

<sup>b</sup> Department of Chemistry, University of Isfahan, Isfahan, 81746-73441, Iran

<sup>c</sup> Department of Biology, Faculty of Sciences, University of Isfahan, Isfahan, Iran

\*To whom corresponding should be addressed: Department of Chemistry, University of Isfahan, Isfahan 81746-73441, Iran.

E-mail: bordbar@chem.ui.ac.ir; Fax: +983136689732; Tel: +983137932710

Anisotropic silver nanoparticles with controlled shape and size were synthesized in a simple, efficient and eco-friendly method using *Taxus baccata* extracts as reducing, capping and stabilizing agents. The monodispersed nanoparticles showed narrow size distribution with the average of 75.1 nm and high stability in aqueous colloidal solutions. Different factors including the concentration and the type of plant extract, the concentration of silver nitrate, pH and temperature were investigated in order to synthesize silver nanoparticles of desired size and shape. Surprisingly, the type of plant extract was the main parameter and affected remarkably the physical, chemical and cytotoxic properties of the nanoparticles. On the basis of AFM and TEM results, the use of aqueous extract led to the synthesis of spherical nanoparticles while stable colloidal silver nanoparticles of hexagonal and truncated triangular shape with characteristic absorption spectrum of 530 and 690 nm, respectively, were synthesized in the presence of high concentrations of ethanolic extract. The strong adsorption of *Taxus* metabolites on the surfaces of nanoparticles was confirmed by FTIR and TGA analysis. The MTT assay revealed potent anticancer effects of aqueous extract nanoparticles on MCF-7 cells with IC<sub>50</sub> value of 0.25 µg mL<sup>-1</sup> after 48 hours incubation time. According to the results, the present reported biogenic method has great potential for simple and efficient development of the novel multifunctional nanoparticles for tracking, imaging, and therapy of the cancer cells.

**Keywords:** Silver nanoparticle, *Taxus baccata*, biogenic synthesis, anticancer, Taxol.

## Introduction

Noble metal nanoparticles display attractive properties including quantum confinement effects, antibacterial activity and large reactive surfaces which found potential applications in catalysis, electronics, optics, environmental and biomedical issues.<sup>1</sup>

Recent advances in the development of simple and efficient synthesis methods have led to the increasing availability of nanostructures with highly controlled size, shape and optical properties and widespread interest for the biotechnological and medical applications such as bioimaging,<sup>2,3</sup> *in vivo* sensing,<sup>4,5</sup> diagnosis,<sup>6,7</sup> and therapy.<sup>8,9</sup>

However, expanding the application of nanomaterials also increased toxicity issues, raising concerns to human health and environment.<sup>10</sup> In order to the successful use of metal nanoparticles and nanocomposites in various applications, we need to consider their structural features such as size, shape, composition and the surface chemistry.<sup>11</sup> In this regard, the surface properties including stabilizing agents and functional groups play critical roles in determining biocompatibility and the fate of the nanoparticles. An appropriate selection of these agents not only improve the performance and quality of the nanoparticles but prevent the undesired effects such as toxicity, aggregation and contamination.<sup>12</sup> Development of the improved and environmentally benign methods is necessary for the design of greener nanomaterials with high reproducibility and purity. In terms of the greener production, one would like to avoid the use of hazardous materials and minimize the production of hazardous byproducts.<sup>13</sup> The general method for the production of metal nanoparticles includes the reduction of metal ions in a solution or in a gas phase with high temperature condition. The three main options for the production of the metal nanoparticles with respect to the green chemistry perspective include the selection of the appropriate solvent as the synthesis medium, the choice of an ecofriendly reduction agent, and the choice of a nontoxic capping agents for the stabilization of the nanoparticles.<sup>11</sup> Development of the green chemistry methods for efficient synthesis of metal nanoparticles by using organisms have drawn remarkable interest in recent years.<sup>14</sup> Biogenic synthesis of metal nanoparticles reduces the environmental issues compared with some of the physicochemical methods and can be used to large scale production of nanoparticles with well-defined size and morphology.<sup>15</sup> Among the organisms, plants seem to be the best candidates and they are suitable for large-scale biosynthesis of nanoparticles with various shapes and sizes.<sup>14</sup> The biomolecules present in the plants include various water soluble metabolites (*e.g.* alkaloids, phenolic compounds, terpenoids) and co-enzymes can be used to reduce metal ions to the nanoparticles in a single-step green synthesis process. The reduction of metal ions in the presence of the plant metabolites could be conducted readily at room temperature and pressure and could be easily expanded to the commercial scales. The organic compounds of plants may act both as reducing and stabilizing agents in the synthesis of nanoparticles.<sup>15,16</sup> The use of biological compounds as a renewable reagents for the synthesis of metal nanoparticles in the ambient temperatures and pressures satisfies many principles of green chemistry.<sup>17</sup> Extracts of different plant species have been successfully used in the synthesis of metal nanoparticles especially silver nanoparticles.

*Taxus* species are known to produce a wide range of natural diterpenoids named as Taxoids or Taxanes, by approximately 350 identified forms.<sup>18</sup> Taxol, as one of the most known Taxoids, is well-established as a potent anticancer agent with powerful effects against a range of cancers.<sup>19</sup> Taxanes (especially paclitaxel and docetaxel) represent an important class of antitumor agents extracted from the yew trees with significant antitumor activity against a broad spectrum of human tumors. Taxanes are cell cycle-specific agents that bind with high-affinity to microtubules,<sup>20</sup> stabilize and enhance tubulin polymerization and suppress spindle microtubule dynamics. This effectively inhibits mitosis, motility, and intracellular transport, leading to the apoptotic cell death.<sup>21,19</sup> Recently there are some reports about antitumor effects of the extracts and other compounds of *Taxus* sp.<sup>22,23</sup> However, further studies is crucial to develop the novel and efficient agents for the improved treatment of cancer patients with cost effective approaches. In this context, finding and investigation of the new Taxanes constitutes in combination with the other treatment agents is one of the most exciting strategies for improving the clinical control of cancer patients especially for the breast cancer.<sup>21</sup>

Treatment of the mammalian cells with silver nanoparticles has been reported to cause the cell cycle arrest in G<sub>2</sub>/M phase possibly due to the repair of damaged DNA. The silver nanoparticles have been known based on the transmission electron microscopic (TEM) analysis to involve directly in the mitochondrial toxicity and DNA damage. It was anticipated that DNA damage is augmented by deposition, followed by interaction of silver nanoparticles to the DNA leading to the cell cycle arrest in the G<sub>2</sub>/M phase.<sup>24</sup> Consequently, it seems that the silver nanoparticles and Taxanes both act on DNA in the nucleus and silver may be an excellent candidate for Taxane delivery to the nucleus of cancer cells. Moreover, the combination treatment of the tumors by silver and Taxanes may cause synergistic cytotoxicity on the cancer cells. With respect to the mentioned hypotheses, in the present work, for the first time, a novel and totally green approach was reported toward the synthesis of stable colloidal silver nanoparticles with potent anticancer properties and controlled size and shape by using different extracts of *Taxus baccata* L.

## Experimental

### Materials

Dulbecco's modified Eagle's medium (DMEM), L-glutamine, Fetal calf serum (FCS), Dimethyl sulfoxide, 3-(4,5-Dimethylthiazol-2-yl)-2,5-Diphenyltetrazolium Bromide (MTT), and Silver nitrate (AgNO<sub>3</sub>), were obtained from Sigma (Germany). Organic solvents for Taxane extraction and HPLC analysis were purchased from Merck (Darmstadt, Germany). A standard of Taxol was prepared by Calbiochem (San Diego, CA, USA) and standards of 10-Deacetylbaccatin III and Baccatin III were obtained from Sigma (Germany). All of the aqueous solutions were prepared by double distilled water.

### Preparation and analysis of the plant extract

Freshly collected *T. baccata* needles from the flower garden of Isfahan, Iran, were dried and powdered. The *Taxus* extract was prepared by suspending 2 grams of the powder in 50 mL double distilled water or ethanol (80% v/v) following by sonication for 1 h. The suspension was then shaken for another 1 h and finally filtered through Whatman No.1 filter paper. Depending on the experimental requirements either the ethanolic or aqueous extract was used.

HPLC analysis was used to confirm the presence of various Taxane compounds in the ethanolic extract according to the literature method with some modifications.<sup>25,26</sup> Briefly, the filtered ethanolic extract was concentrated to dryness in a rotary evaporator at 75 °C and the residue was dissolved in 2 mL methanol and degreased by adding 1 mL water for 4 h. The filtered methanolic extracts were analyzed by reverse phase HPLC (Sykam, Eresing, Germany) with UV detection at 227 nm. A 20 µL portion of the samples was injected on to a reverse-phase column (Kromasil C18, 250 mm × 4.6 mm). The mobile phase consisted of isocratic (at constant concentration) methanol/water (70:30, v/v) with flow rate of 1 mL min<sup>-1</sup>.

### Synthesis of silver nanoparticles

Different parameters including the concentration and type of the plant extract, the concentration of silver nitrate, temperature and pH of the reaction were systematically investigated in order to optimize the synthesis of stable colloidal silver nanoparticles with controlled size and shape. Different reaction conditions, used for the synthesis of silver nanoparticles by using *Taxus* extracts, are shown in Table 1. All the reactions were performed in the final volume of 20 mL in 100 mL flasks as follows: Appropriate volumes of *Taxus* extract according to Table 1 were mixed with suitable volumes of double distilled water at desired temperature. The pH of resulted solution was adjusted, subsequently, and the appropriate amounts of 10 mM silver nitrate was added drop wise to it under sonication. The reaction was incubated at 10 and 30 °C and the reduction of Ag<sup>+</sup> ions was monitored periodically at different time intervals over a 6 months period by measuring the UV–Vis spectrum of the reaction media using Biochrom WPA UV/Visible spectrophotometer (model Biowave II, UK) in the range between 300 and 800 nm. The corresponding concentrations of plant extracts in NaNO<sub>3</sub> solutions were used as blank. The effect of different pH (3, 5, 7, 9 and 11) on the synthesis of silver nanoparticles was subsequently investigated after optimization of the aforementioned parameters.

### Material characterizations

To investigate the optical properties of final products, the nanoparticles were isolated by centrifugation after completion of the reaction, dispersed in water and used for UV–Vis Spectroscopy. TEM images were recorded on a CM30 electron microscope (Philips, Eindhoven, Netherlands) operating at an accelerating voltage of 100-300 kV. The samples were prepared by drop coating colloidal solution of silver nanoparticles onto a hydrophilic carbon coated copper grid and allowed to air dry. The qualitative chemical composition of the colloidal nanoparticles and dried extract were analyzed by energy dispersive X-ray

spectroscopy (EDS) using a Bruker Quantax 200 detector (Bruker AXS Inc., Madison, WI, USA). Samples of the biogenic silver nanoparticles were also analyzed by an atomic force microscopy (AFM, contact mode on a DualScope™ scanning probe-optical microscope, DME equipped with a C-26 controller) through solution casting onto highly oriented glass slides. To estimate the particle size distribution and zeta potential of the nanoparticles, the colloidal solutions of nanoparticles were analyzed by using ZEN 3600 Zetasizer (Malvern, Worcestershire, UK). To perform FTIR analysis, different colloidal solutions of silver nanoparticles were centrifuged at 15,000 rpm for 15 min and the pellets were completely dried via a freeze dryer (VaCo 5, Zirbus, Germany) and analyzed. Another sample subjected to FTIR analysis after washing the pellet for one hour in ethanol solution (70% v,v) and drying by freeze dryer. *T. baccata* needles were also dried, powdered and analyzed as control. For FTIR analysis, the samples were mixed with KBr powder and pelletized and finally the spectra were recorded using FT/IR-6300 Spectrometer (Jasco, Japan) with wavelength range between 4000  $\text{cm}^{-1}$  and 400  $\text{cm}^{-1}$ . Thermogravimetric analysis (TGA) was conducted using a Mettler TG50 (Switzerland) at a constant heating rate of 10  $^{\circ}\text{C min}^{-1}$  from 25  $^{\circ}\text{C}$  to 700  $^{\circ}\text{C}$  under nitrogen atmosphere.

#### Cell viability assay

The cell viability was evaluated for MCF-7 human breast cancer cell line via MTT assay. Briefly, MCF-7 cells were grown in DME medium supplemented with 10% FCS and 1 mM L-glutamine. The cells were seeded on 96-well plates containing 200  $\mu\text{L}$  medium at a density of  $10^4$  cells  $\text{mL}^{-1}$  and cultured in a humidified incubator at 37  $^{\circ}\text{C}$  with 5%  $\text{CO}_2$  overnight. To evaluate anticancer activity of the silver nanoparticles synthesized by aqueous or ethanolic extracts, the cultured cells were treated in separate wells with different concentrations of silver nanoparticles (0.25, 1.25, 2.5, 5, 7.5, 10 and 20  $\mu\text{g mL}^{-1}$ ) and for different time periods (48 and 72 h). Then the medium was discarded and 100  $\mu\text{L}$  MTT (0.5  $\text{mg mL}^{-1}$  in media) was added into each well and incubated again at 37  $^{\circ}\text{C}$  for 4 h. Subsequently, 150  $\mu\text{L}$  DMSO was added to each well and the absorbance was measured immediately at 570 nm by using microplate reader. Three independent experiments were conducted for each toxicity endpoint. The cell viability was determined as ratio of absorbance values from each treatment and the control. To investigate the anticancer activity of the ethanolic and aqueous extracts on MCF-7 cells, corresponding concentrations of *Taxus* extracts were also used individually in control experiments. Cytomorphological changes of MCF-7 cells were also investigated by optical microscopy. Briefly, the cells were seeded at a density of  $1 \times 10^6$  cells  $\text{mL}^{-1}$  in 24-well plate and incubated in a humidified incubator at 37  $^{\circ}\text{C}$  with 5%  $\text{CO}_2$  overnight. Following exposure to the different concentrations of silver nanoparticles for appropriate times (24, 48 or 72 h), the cells were washed with PBS and imaged.

## Results and discussion

### Biogenic synthesis of colloidal silver nanoparticles

In order to synthesize stable colloidal silver nanoparticles with narrow size distribution and appropriate physical properties, the reaction conditions were initially optimized. UV-Vis spectroscopy was used to follow the reactions process and characterize the optical properties of produced nanoparticles.

The solvent used for the extraction of metabolites and also the concentration of plant extract were found to have the greatest effects on the shape, size distribution and optical properties of silver nanoparticles. While the spherical nanoparticles were obtained by using aqueous extract of *T. baccata*, the use of ethanolic extract led to the synthesis of anisotropic nanoparticles. This observation can be attributed to the different concentrations and combinations of the organic compounds present in the extracts which may act both as reducing and stabilizing agents in the synthesis of silver nanoparticles.<sup>27</sup> Water has been commonly used as solvent to extract water soluble metabolites for the reduction of metal ions to nanoparticles. Regarding to the polarity and solubility of Taxane compounds, selection of the appropriate solvent can seriously affect the extraction yield of the metabolites. Based on the previous studies,<sup>26,28</sup> a 80% ethanol solution was used in this study as an suitable solvent for the efficient extraction of Taxoids from *Taxus* cells. According to the water insolubility of Taxanes, a comparison between ethanolic and aqueous extracts of *Taxus* in terms of the synthesis of silver nanoparticles may help to elucidate the role of Taxane diterpenoids in the synthesis and stabilization of the nanoparticles and controlling their size and shape. HPLC analysis of the ethanolic extract indicated the presence of main Taxoids including 10-Deacetylbaaccatin III, Baaccatin III and Taxol (Fig. 1).

The color of the solution changed from light yellow to light brown as the reaction progressed in the presence of aqueous extract and UV-Vis spectroscopy showed only one symmetric absorption peak at 420 nm (Fig. 2) which is the characteristic surface plasmon resonance of spherical silver nanoparticles.<sup>29</sup> By increasing the concentration of aqueous extract, the plasmon absorption maximum shifted slightly towards longer wavelengths, which is an indication of particle size increasing (Fig. 2).<sup>29</sup> Actually, decreasing the concentration of aqueous extract led to the slower reduction and synthesis of the spherical nanoparticles with more limited size distribution, higher stability in colloids and sharper absorption spectrum (Fig. 2). In general, the nanoparticles synthesized in the presence of the aqueous extract were spherical and relatively unstable. The application of water as solvent mainly led to the extraction of polysaccharides which serve as either reducing or capping agents and in some cases act the both roles in the synthesis of nanoparticles.<sup>1</sup> Spherical silver nanoparticles with relatively limited distribution size of the average 91.2 nm and Zeta potential value of -7.77 were obtained in the optimum condition in the presence of 1 mL aqueous extract and 0.5 mM silver nitrate (Fig. 2).

It seems that water-soluble metabolites present in *T. baccata* needles are mainly involved in reducing silver ions to silver nanoparticles but the use of ethanol solution resulted to the extraction of different compounds that may act as both reducing and capping agents. The reaction rate is considerably slower in the presence of ethanolic extract and can be controlled by the

concentration of the extract. The silver colloids which were obtained in the presence of low concentration of ethanolic extract are predominantly well-dispersed spherical nanoparticles and a few faceted nanodisks can also be seen from the TEM image (Fig. 3a). By increasing the concentration of ethanolic extract, the reaction rate decreased considerably and the majority of synthesized nanoparticles became hexagonal nanodisks (Fig. 3b) with average hydrodynamic diameter of 75 nm which confirmed by the AFM analysis (Fig. 4). The absorption spectrum of these colloidal nanoparticles exhibits two peaks at 420 and 530 nm (Fig. 3b) correspond to the transverse and longitudinal plasmon modes.<sup>30,31,32</sup> In high concentration of the ethanolic extract, the reaction progress was very slow and need a few days to change the color of the solution from light green to greenish brown. Moreover, a small percentage of truncated triangular nanoparticles have also been observed together with hexagonal nanodisks in this condition and a new red-shifted peak was observed at 690 nm (Fig. 3c) which is the characteristic surface plasmon resonance of these nanoparticles<sup>29</sup>. The presence of elemental metal signal was confirmed by energy dispersive spectroscopy (EDS) of the silver nanoparticles. The silicon signal may be related to the glass slide used in the EDS analysis of colloidal nanoparticles (Fig. 5). The comparison of the EDS results of pure extract (Fig. S1) and silver nanoparticles (Fig. 5) represents that all other signals related to the organic compounds of plant extract or nitrate substrate. However, the silicon signal is not observed in Fig. S1 that is due to the using of double sided adhesive tape instead of glass slide. The anisotropic silver nanoparticles with narrow particle size distribution and average size value of 75.1 nm and polydispersity index (PDI) of 0.27 were found stable in solution with Zeta potential value of -16.4 over 6 months. A thin layer of the organic compounds was clearly observed around the nanoparticles in TEM images indicating the efficient role of the metabolites as capping agents in the synthesis of stable silver nanoparticles. The exact role of the organic compounds in controlling the nanoparticle shape is still unclear. One possible function was to kinetically control the growth rates of various faces by interacting with these faces through adsorption and desorption.<sup>33</sup> Similar results have been reported by Shankar *et al.*<sup>34,35</sup> for the synthesis of silver and gold nanoparticles in the presence of terpenoids. He *et al.*,<sup>36</sup> also previously reported the synthesis of silver nanoparticles of different shapes and sizes in different solvents as reaction medium under microwave irradiation from a solution of silver nitrate in the presence of poly(*N*-vinyl-2-pyrrolidone). *T. baccata* needles are rich in diterpenoids especially Taxanes which possibly act as capping agents and can affect the shape and stability of the nanoparticles. Kumar and Yadav<sup>27</sup> reported earlier that the source of plant extract affect the characteristics of the nanoparticles. In contrast with the previous results reported by Jin *et al.*<sup>37</sup> who stated photoinduced conversion of spherical silver nanoparticles to nanoprisms in the presence of NaBH<sub>4</sub> as reducing agent and Bis (*p*-sulfonatophenyl) phenylphosphine dihydrate dipotassium (BSPP) as stabilizing agent, the biogenic synthesis method reported here is not dependent on light and can also be performed in the dark condition with less speed. Thus, the shape and size of the silver nanoparticles can be controlled by varying the two parameters of type and amount of *Taxus* extract in the synthesis reaction medium. Similar results have been reported previously by Shankar *et al.*,<sup>38,39</sup> in terms of controlling the edge length of triangular gold nanotriangles synthesized by lemongrass extract.

Increasing the concentration of silver nitrate above 1 mM caused to rapid reduction of silver nitrate following by agglomeration and precipitation of the nanoparticles. The results also showed that pH had a substantial effect on the physical properties of the nanoparticles as well as the rate of reaction. The faster reaction was observed after increasing pH up to 10 and the nanoparticles were also found more stable than in the case of acidic conditions. Adjusting the pH values of the reactions below 4 even in the presence of high concentration of ethanolic extract resulted in the synthesis of spherical nanoparticles with maximum absorption peak around 400 nm that the particles aggregated and precipitated after a few days. On the other hands, conducting the reaction in the pH between 6 and 8 led to the synthesis of stable colloidal nanoparticles with different shape and optical properties. Similar results were reported by Blanco-Andujar *et al.*,<sup>40</sup> and Kaler *et al.*,<sup>41</sup> who stated that the change in pH can affect the nanoparticle synthesis and morphology. Although, the increasing of temperature enhances the reaction rate and reduces nanoparticle stability, it does not have any significant effect on the shape of nanoparticles, however, it decreases the average particle size that is in agreement with previous reports.<sup>42,43</sup>

#### Chemical analysis of the nanoparticle surfaces

Fourier transform spectroscopy (FTIR) and Thermogravimetric analysis (TGA) were used to initially determine the bioorganic compounds bound to the surfaces of the silver nanoparticles.<sup>17</sup> To identify which functional groups from the leaf extracts take part in the reaction as reducing and capping agents, FTIR analysis was carried out for aqueous and ethanolic extracts and also for dry leaf powder of *T. baccata*. The spectrum of the silver nanoparticles and dry leaf powder were compiled. As indicated in Fig. 6, the FTIR spectrum of *T. baccata* leaf powder showed several sharp absorption peaks located at 3370 cm<sup>-1</sup>, 3300 cm<sup>-1</sup>, 2925 cm<sup>-1</sup>, 1735 cm<sup>-1</sup>, 1654 cm<sup>-1</sup>, 1606 cm<sup>-1</sup>, 1545 cm<sup>-1</sup>, 1446 cm<sup>-1</sup>, 1375 cm<sup>-1</sup>, 1245 cm<sup>-1</sup>, 1053 cm<sup>-1</sup> and 829 cm<sup>-1</sup>.

Most of these peaks which present in the spectra could be an indication of the efficient adsorption of the plant extracts on the surfaces of silver nanoparticles which may be attributed to the aliphatic, aromatic and also protein structures. As illustrated in Fig. 6, there is a negligible difference between the extracts during the preparation of the nanoparticles.

The aforementioned results, approved that the synthesized silver nanoparticles by *T. baccata* extracts could be encapsulated by some fractions such as proteins and other metabolites (especially terpenoids such as Taxol having functional groups of amines, aldehydes, carboxylic acid, and alcohols).

The thermal stability of organic compounds on the nanoparticle surfaces was determined using TGA analysis. The weight loss of silver nanoparticles synthesized using ethanolic extract of *T. baccata* was 27% when the sample was heated from 0 to 521 °C. There was another weight loss of 8.3% when the temperature was increased up to 678 °C. The total weight loss of about 36.89% resulted after increasing the temperature up to 700 °C. The weight loss is attributed to the degradation of bioorganic compounds present on the surface of the nanoparticles.

It has been reported that the type of capping agent determines the potency of silver nanoparticles.<sup>44</sup> The capping agents can stabilize the nanoparticles by avoiding the aggregation of the particle as well as the interactions of the particles with *in vivo* components and also restores their activities.

With respect to the FTIR results of washed nanoparticles by ethanolic solution and also their TGA analysis at high temperatures that is an indication of the stable adsorption of organic compounds on the silver nanoparticles, it can be claimed the suitability of these nanoparticles for efficient and safe transferring organic compounds to the cancerous cells with minimum side effects.

### **Anticancer activity**

An exhaustive MTT assay on MCF-7 cells was conducted to evaluate anticancer activity of the synthesized silver nanoparticles in different doses and exposure times. Significant differences in the viability of MCF-7 cells were observed in the presence of different concentrations of silver nanoparticles and for different exposure times (Fig. 7). The results represent the enhancement of cytotoxic activity with the increasing of silver nanoparticle concentration and exposure time. Although, both synthesized silver nanoparticles by using ethanolic and aqueous extracts showed significant anticancer activity, surprisingly, the synthesized nanoparticles in the presence of aqueous extract demonstrated superior anticancer effects. This result is in contrary to our expectation regards to more efficient extraction of Taxane compounds in ethanol. This may be referred to the more effective anticancer activity of water soluble *Taxus* metabolites when used as reducing and capping agents for the synthesis of silver nanoparticles.

The obtained IC<sub>50</sub> values after 48 hours incubation time are 0.25 and 5 µg mL<sup>-1</sup> for synthesized silver nanoparticles by aqueous and ethanolic extracts, respectively. Significant mortality (up to 97%) was observed after this incubation time with 5 µg mL<sup>-1</sup> of aqueous extract synthesized silver nanoparticles and higher concentrations led to the complete mortality of the cells. The cytotoxicity effects of the nanoparticles increased by the increasing of exposure time as more than 50% of the cells were died after incubation for 72 hours by all the doses.

The corresponding concentrations of *Taxus* extracts were individually used to investigate the anticancer activity of the aqueous and ethanolic extracts on MCF-7 cells as control experiments. The maximum mortalities of 49.54 and 47.26% were obtained after 48 hours incubation in the highest concentration of ethanolic and aqueous extracts, respectively. This represents the moderate anticancer activity of the extracts (the results were shown in Fig. S2). Hence, with respect to the potent anticancer activity of biogenic silver nanoparticles, it can be concluded that the coating of silver nanoparticles with *Taxus* extracts displays synergistic anticancer effects.

Optical microscopic studies of MCF-7 cells showed morphological changes following with the suppression of cell growth and finally the cell clumping and death (Fig. 8) due to the exposure to the biogenic silver nanoparticles.

The results show higher anticancer activity of the synthesized silver nanoparticles by *Taxus* extracts in comparison with other studied plant extracts. *e.g.*, Kaler *et al.*,<sup>41</sup> reported the IC<sub>50</sub> value of 10 µg mL<sup>-1</sup> for the silver nanoparticles synthesized by *S. boulardii*, cytotoxic effect (up to 94.02%) at 500 µg mL<sup>-1</sup> concentration of silver nanoparticles synthesized by *Piper longum* leaf extracts was reported by Jacob *et al.*,<sup>45</sup> and complete mortality rate of MCF-7 cells was also observed in 50 µg mL<sup>-1</sup> concentration of the silver nanoparticles synthesized in the presence of *Sesbania grandiflora* leaf extract.<sup>46</sup>

Various factors including the composition, size, shape, surface charge, and capping molecules are known to affect the cytotoxicity of nanoparticles.<sup>47</sup> Our results demonstrated that the biologic compounds used as reducing and capping agents of metal nanoparticles play a critical role in cytotoxicity of nanoparticles and their potential interactions with tumor cells.

## Conclusions

The ability to modulate the shape, size and optical properties of the synthesized silver nanoparticles in the presence of ethanolic extract of *Taxus baccata* in optimum reaction conditions which reported here, may have potential to introduce a novel and exciting green synthesis approach toward the development of a new generation of nanostructures with controlled physical and chemical properties. The other, and perhaps most important advantage of this approach includes the possibility to obtain stable silver nanoparticles with potent anticancer activity simultaneously via a simple and cost effective manner. The absorption spectrum of nanoparticles can be tuned, by carefully optimizing the synthesis conditions, to the near infrared (NIR) region which eliminate the interference from tissue autofluorescence and hence, the resulted nanoparticles also have great potential for deep tissue imaging and tumor targeting. In conclusion, the biosynthesized silver nanoparticles may have potential to use as multifunctional nanoparticles for different applications such as diagnosis, targeting, drug delivery and imaging of the tumors simultaneously. Further studies in order to surface engineering, targeting and bioconjugation of the silver nanoparticles may be useful to develop novel nanoparticles for different targets especially biomedical and biotechnological issues.

## Acknowledgement

The financial support of research council of Isfahan University is gratefully acknowledged.

## References

- 1 F. Cheng, J. W. Betts, S. M. Kelly, J. Schaller and T. Heinze, *Green Chem.*, 2013, **15**, 989–998.
- 2 L. Liu, R. Hu, W. C. Law, I. Roy, J. Zhu, L. Ye, S. Hu, X. Zhang and K. T. Yong, *Analyst*, 2013, **138**, 6144–6153.
- 3 C. Chien, H. Chen, S. Lai, K. Wu, X. Cai, Y. Hwu, C. Petibois, Y. Chu and G. Margaritondo, *J. Nanobiotechnology*, 2012, **10**, 10.
- 4 K. J. Lee, P. D. Nallathamby, L. M. Browning, C. J. Osgood and X. H. N. Xu, *ACS Nano*, 2007, **1**, 133–143.
- 5 D. van Lierop, Ž. Krpetić, L. Guerrini, I. Larmour, J. Dougan, K. Faulds and D. Graham, *Chem. Commun. (Camb)*, 2012, **48**, 8192–8194.
- 6 I. H. El-Sayed, X. Huang and M. El-Sayed, *Nano Lett.*, 2005, **5**, 829–834.
- 7 X. Huang, I. H. El-Sayed, W. Qian and M. El-Sayed, *Nano Lett.*, 2007, **7**, 1591–1597.
- 8 T. R. Kuo, V. Hovhannisyanyan, Y. C. Chao, S. L. Chao, S. J. Chiang, S. J. Lin, C. Y. Dong and C. C. Chen, *J. Am. Chem. Soc.*, 2010, **132**, 14163–14171.
- 9 J. R. Hwu, Y. S. Lin, T. Josephrajan, M. H. Hsu, F. Y. Cheng, C. S. Yeh, W. C. Su and D. B. Shieh, *J. Am. Chem. Soc.*, 2009, **131**, 66–68.
- 10 M. V. D. Z. Park, A. M. Neigh, J. P. Vermeulen, L. J. J. Fonteyne, H. W. Verharen, J. J. Briedé, H. van Loveren and W. H. de Jong, *Biomaterials*, 2011, **32**, 9810–9817.
- 11 P. Raveendran, J. Fu and S. L. Wallen, *J. Am. Chem. Soc.*, 2003, **125**, 13940–13941.
- 12 J. Virkutyte and R. S. Varma, *Chem. Sci.*, 2011, **2**, 837–846.
- 13 J. E. Hutchison, *ACS Nano*, 2008, **2**, 395–402.
- 14 S. Iravani, *Green Chem.*, 2011, **13**, 2638–2650.
- 15 A. K. Mittal, Y. Chisti and U. C. Banerjee, *Biotechnol. Adv.*, 2013, **31**, 346–356.
- 16 D. Mubarak Ali, N. Thajuddin, K. Jeganathan and M. Gunasekaran, *Colloids Surf. B. Biointerfaces*, 2011, **85**, 360–365.
- 17 W. Liang, T. L. Church and A. T. Harris, *Green Chem.*, 2012, **14**, 968–975.
- 18 A. Abbasi Kejani, S. A. Hosseini Tafreshi, S. M. Khayyam Nekouei and M. R. Mofid, *Mol. Biol. Rep.*, 2010, **37**, 797–800.
- 19 N. Desai, V. Trieu, Z. Yao, L. Louie, S. Ci, A. Yang, C. Tao, T. De, B. Beals, D. Dykes, P. Noker, R. Yao, E. Labao, M. Hawkins and P. Soon-Shiong, *Clin. Cancer Res.*, 2006, **12**, 1317–1324.
- 20 D. G. I. Kingston and J. P. Snyder, *Acc. Chem. Res.*, 2014, DOI:10.1021/ar500203h.
- 21 E. Miele, G. P. Spinelli, E. Miele, F. Tomao and S. Tomao, *Int. J. Nanomedicine*, 2009, **4**, 99–105.
- 22 C. Yan, Y. Yin, D. Zhang, W. Yang and R. Yu, *Carbohydr. Polym.*, 2013, **96**, 389–395.

- 23 W. Shang, J. Qiao, C. Gu, W. Yin, J. Du, W. Wang, M. Zhu, M. Han and W. Lu, *BMC Complement. Altern. Med.*, 2011, **11**, 123.
- 24 P. V Asharani, G. Low, K. Mun, M. P. Hande and S. Valiyaveetil, *ACS Nano*, 2009, **3**, 279–290.
- 25 A. Abbasi Kajani, S. Moghim and M. R. Mofid, *Biotechnol. Appl. Biochem.*, 2012, **59**, 223–227.
- 26 S. Li, Y. Fu, Y. Zu, R. Sun, Y. Wang, L. Zhang, H. Luo, C. Gu and T. Efferth, *J. Pharm. Biomed. Anal.*, 2009, **49**, 81–89.
- 27 V. Kumar and S. K. Yadav, *J. Chem. Technol. Biotechnol.*, 2009, **84**, 151–157.
- 28 H. Luo, Y. K. Nie, Y. J. Fu, Y. G. Zu, S. M. Li, W. Liu, L. Zhang, M. Luo, Y. Kong and Z. N. Li, *J. Sep. Sci.*, 2009, **32**, 192–201.
- 29 J. J. Mock, M. Barbic, D. R. Smith, D. Schultz and S. Schultz, *J. Chem. Phys.*, 2002, **116**, 6755–6759.
- 30 M. Maillard, P. Huang and L. Brus, *Nano Lett.*, 2003, **3**, 1611–1615.
- 31 E. Hao, K. L. Kelly, J. T. Hupp and G. C. Schatz, *J. Am. Chem. Soc.*, 2002, **124**, 15182–15183.
- 32 K. L. Kelly, E. Coronado, L. L. Zhao and G. C. Schatz, *J. Phys. Chem. B*, 2003, **107**, 668–677.
- 33 Y. Sun, B. Gates, B. Mayers and Y. Xia, *Nano Lett.*, 2002, **2**, 165–168.
- 34 S. S. Shankar, A. Rai, A. Ahmad and M. Sastry, *J. Colloid Interface Sci.*, 2004, **275**, 496–502.
- 35 S. S. Shankar, A. Ahmad, R. Pasricha and M. Sastry, *J. Mater. Chem.*, 2003, **13**, 1822–1826.
- 36 R. He, X. Qian, J. Yin and Z. Zhu, *J. Mater. Chem.*, 2002, **12**, 3783–3786.
- 37 R. Jin, Y. Cao, C. Mirkin, K. L. Kelly, G. C. Schatz and J. G. Zheng, *Science*, 2001, **294**, 1901–1903.
- 38 S. Shankar, A. Rai, A. Ahmad and M. Sastry, *Chem. Mater.*, 2005, **11**, 566–572.
- 39 S. S. Shankar, A. Rai, B. Ankamwar, A. Singh, A. Ahmad and M. Sastry, *Nat. Mater.*, 2004, **3**, 482–488.
- 40 C. Blanco Andujar, D. Ortega, Q. Pankhurst and N. T. K. Thanh, *J. Mater. Chem.*, 2012, **22**, 12498–12506.
- 41 A. Kaler, S. Jain and U. C. Banerjee, *Biomed Res. Int.*, 2013, 872940.
- 42 J. Y. Song, H. K. Jang and B. S. Kim, *Process Biochem.*, 2009, **44**, 1133–1138.
- 43 J. Y. Song and B. S. Kim, *Bioprocess Biosyst. Eng.*, 2009, **32**, 79–84.
- 44 D. P. Gnanadhas, M. Ben Thomas, R. Thomas, A. M. Raichur and D. Chakravorty, *Antimicrob. Agents Chemother.*, 2013, **57**, 4945–4955.
- 45 S. J. P. Jacob, J. S. Finub and A. Narayanan, *Colloids Surf. B. Biointerfaces*, 2012, **91**, 212–214.
- 46 M. Jeyaraj, G. Sathishkumar, G. Sivanandhan, D. Mubarak Ali, M. Rajesh, R. Arun, G. Kapildev, M. Manickavasagam, N. Thajuddin, K. Premkumar and A. Ganapathi, *Colloids Surf. B. Biointerfaces*, 2013, **106**, 86–92.
- 47 A.K.Suresh,D.Pelletier,W.Wang,J.L.Morrell-Falvey,B.GuandM.J.Doktycz,*Langmuir*,2012,**28**,2727–2735.

**Table 1.** Synthetic conditions for the preparation of stable aqueous colloidal solutions of silver nanoparticles by using *T. baccata* extracts.

	AgNO <sub>3</sub> (mM)	Extract type	Extract volume	Temperature (°C)
1	0.5	Ethanollic, Aqueous	1 mL	10, 30
2	1	Ethanollic, Aqueous	1 mL	10, 30
3	0.5	Ethanollic, Aqueous	2 mL	10, 30
4	1	Ethanollic, Aqueous	2 mL	10, 30
5	0.5	Ethanollic, Aqueous	3 mL	10, 30
6	1	Ethanollic, Aqueous	3 mL	10, 30
7	0.5	Ethanollic, Aqueous	4 mL	10, 30
8	1	Ethanollic, Aqueous	4 mL	10, 30
9	0.5	Ethanollic, Aqueous	5 mL	10, 30
10	1	Ethanollic, Aqueous	5 mL	10, 30

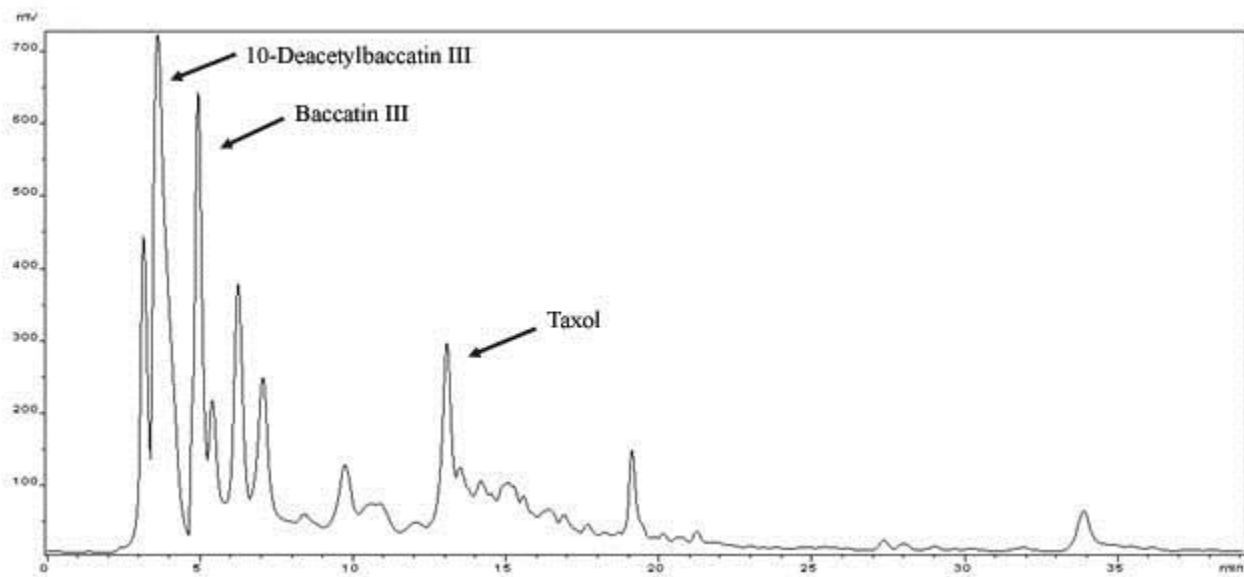


**Fig. 1** HPLC chromatogram of the ethanolic extract of *T. baccata* L.

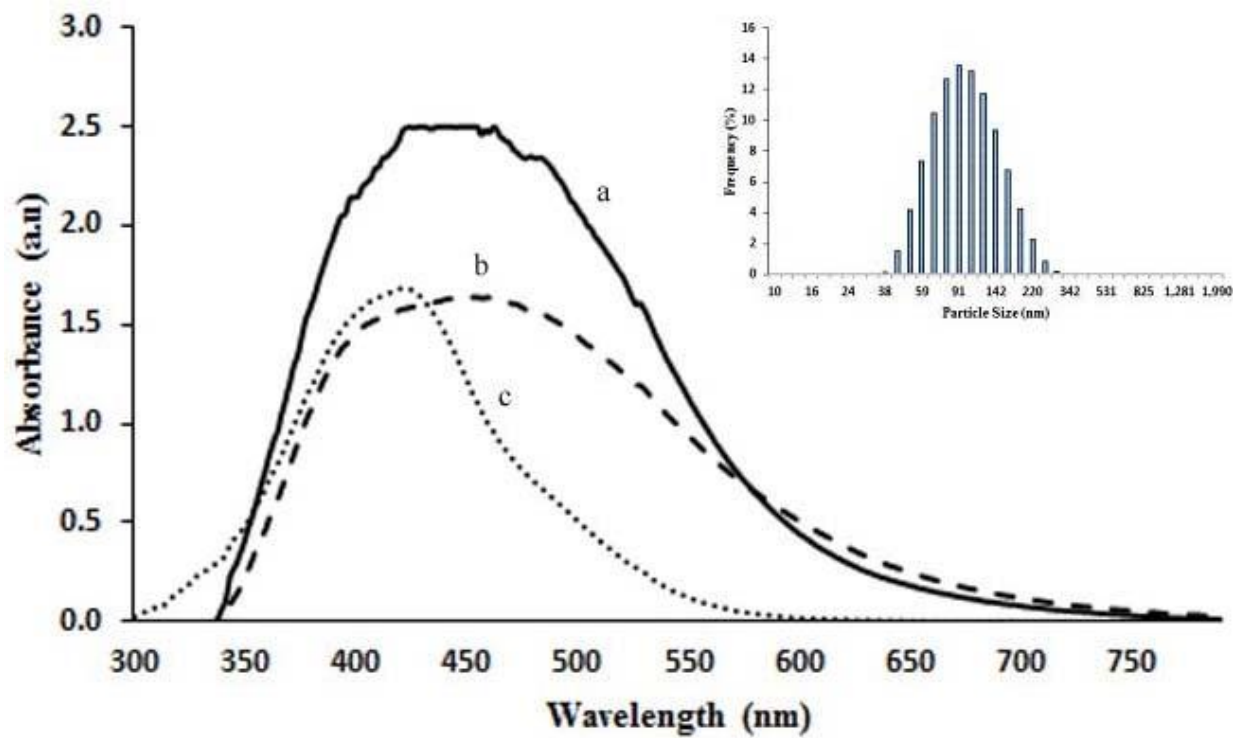


**Fig. 2** UV-Vis spectra of the silver nanoparticles synthesized in the presence of high (a), medium (b) and low (c) concentration of aqueous extract. Corresponding particle size distribution of the curve c is shown as inset curve.

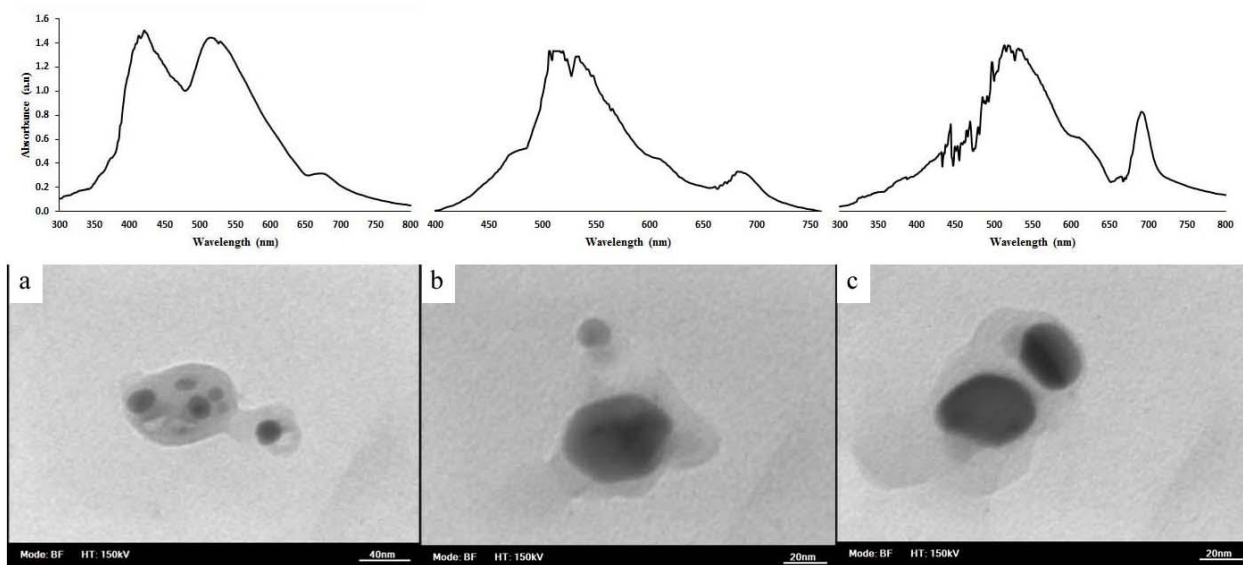


**Fig. 3** TEM images (below) and corresponding UV-Vis spectrum (above) for the silver nanoparticles synthesized in the presence of 1 mL (a), 3 mL (b) and 5 mL (c) of ethanolic extract (All the reactions were performed in the final volume of 20 mL and pH 7).

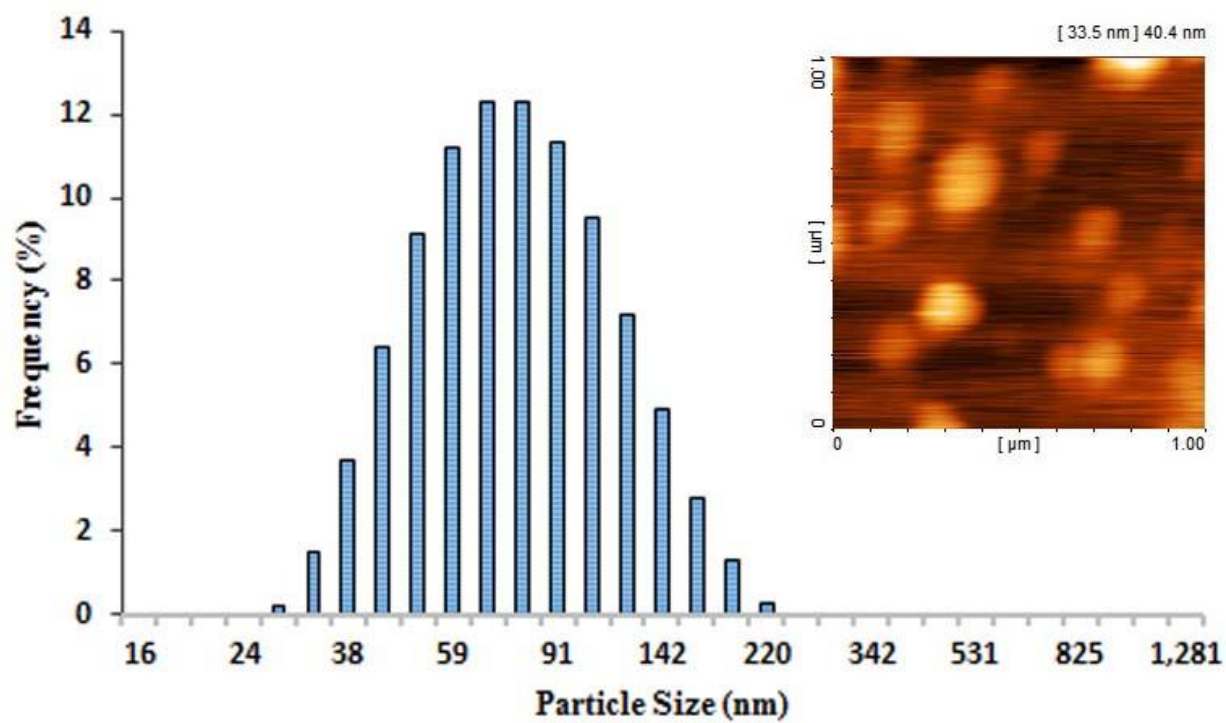


**Fig. 4** Particle size distribution and AFM result for the anisotropic silver nanoparticles synthesized in the presence of high concentration of ethanolic extract.

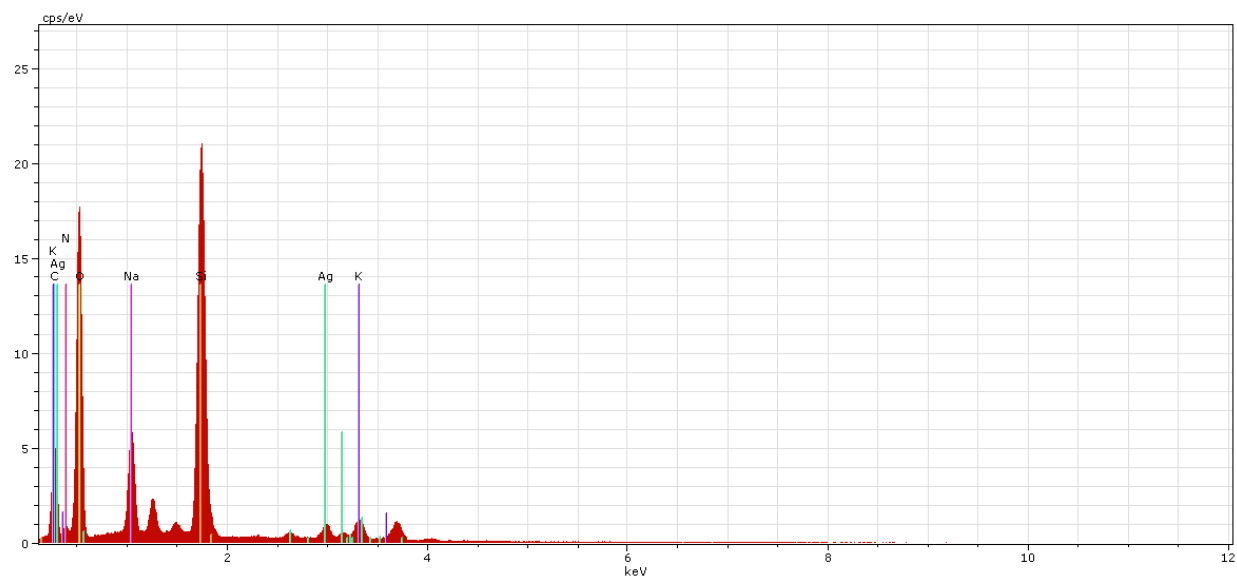


**Fig. 5** EDS spectra of silver nanoparticles synthesized by ethanolic extract of *T. baccata* L.

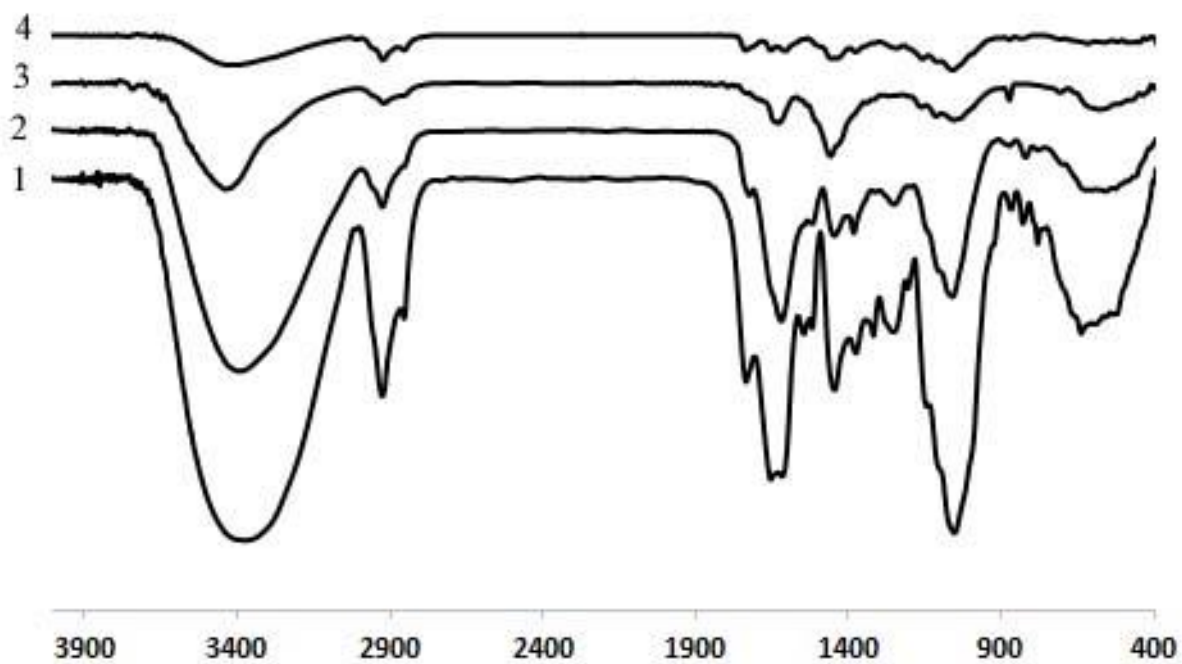


**Fig. 6** FTIR spectra of dried powder of *T. baccata* needles (curve 1); silver nanoparticles synthesized by reduction of silver ions with aqueous extract of *T. baccata* (curve 2); silver nanoparticles synthesized in the presence of ethanolic extract and after washing with ethanol solution for 1 h (curve 3) and silver nanoparticles synthesized by reduction of silver ions with ethanolic extract of *T. baccata* (curve 4).

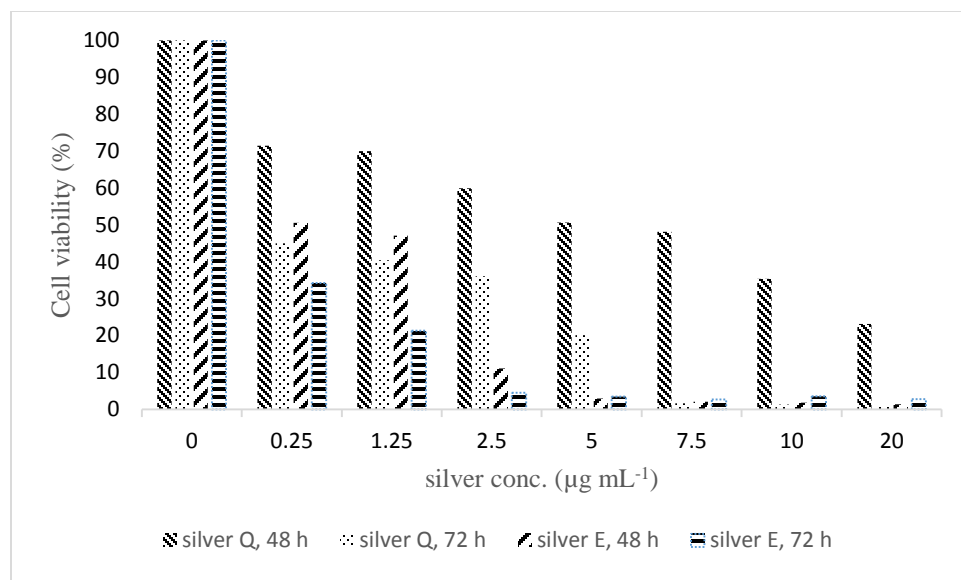


**Fig. 7** Viability percentage of the MCF-7 cells after incubation for different periods (48 and 72 h) with different concentrations of the silver nanoparticles synthesized in the presence of ethanolic (silver E) or aqueous (silver Q) extracts.

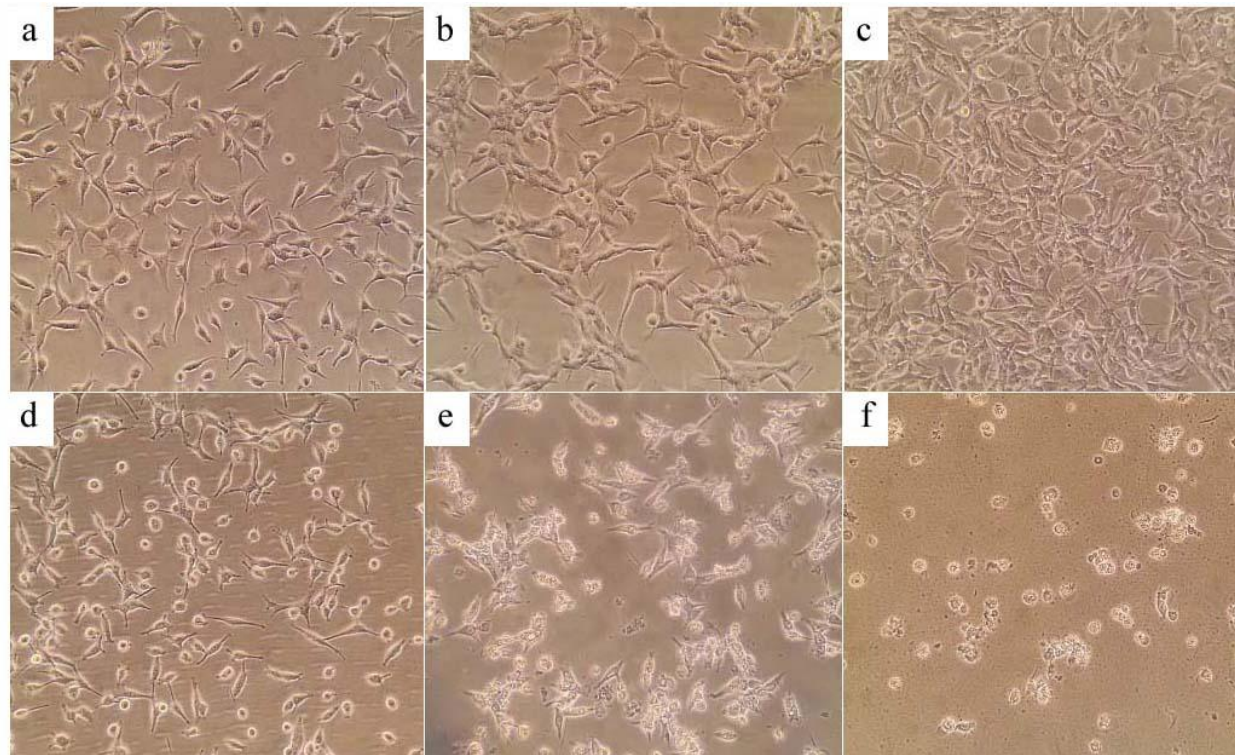


**Fig. 8** Morphological changes of MCF-7 cells after incubation with biogenic silver nanoparticles for 24 (d), 48 (e) and 72 hours (f). Figures a, b and c show MCF-7 cells in the normal culture conditions after 24, 48 and 72 hours, respectively.